applied sciences

MDPI

Article

Instrumental Gait Analysis and Tibial Plateau Modelling to Support Pre- and Post-Operative Evaluations in Personalized High Tibial Osteotomy

Claudio Belvedere [1,*], Harinderjit Singh Gill [2], Maurizio Ortolani [1], Nicoletta Sileoni [1], Stefano Zaffagnini [3], Fabio Norvillo [4], Alisdair MacLeod [2], Giacomo Dal Fabbro [3], Alberto Grassi [3] and Alberto Leardini [1]

[1] Movement Analysis Laboratory, IRCCS Istituto Ortopedico Rizzoli, 40136 Bologna, Italy; maurizio.ortolani@ior.it (M.O.); nicoletta.sileoni@gmail.com (N.S.); leardini@ior.it (A.L.)
[2] Department of Mechanical Engineering, Centre for Therapeutic Innovation, University of Bath, Bath BA2 7AY, UK; rg433@bath.ac.uk (H.S.G.); a.macleod@bath.ac.uk (A.M.)
[3] II Clinical Department, IRCCS Istituto Ortopedico Rizzoli, 40136 Bologna, Italy; stefano.zaffagnini@unibo.it (S.Z.); giacomo.dalfabbro@studio.unibo.it (G.D.F.); alberto.grassi@ior.it (A.G.)
[4] Diagnostic and Interventional Radiology, IRCCS Istituto Ortopedico Rizzoli, 40136 Bologna, Italy; fabio.norvillo@ior.it
* Correspondence: belvedere@ior.it

Featured Application: The inclusion of gait analysis, suitably combined with anatomical modelling derived from patient-specific medical imaging, may lead in the near future to more robust post-operative evaluations of personalized HTO to support the efficacy of this surgical technique, as well as innovative and more biomechanically based pre-operative planning.

Abstract: High tibial osteotomy (HTO) is intended to treat medial knee osteoarthritis by realigning the joint such that the loading in the knee during functional activity shifts laterally. The aim of this study was to use a novel methodology combining motion analysis and 3D modelling to assess the efficacy of this surgery in changing the loading location in the knee in a cohort of 25 patients treated with personalized HTO. Pre-operatively and at 6 months post-surgery, weight-bearing CT and gait analysis during level walking were performed on all patients, as well as clinical evaluations using KOOS and VAS scores. CT scans were used to generate a knee bone model and a virtual tibial plateau plane; the intersection pattern between this plane and the ground reaction force (GRF) vector was calculated in the pre- and post-operative gait analyses. Clinical scores improved significantly ($p < 0.001$) after surgery (pre-/post-operative KOOS and VAS: 56.2 ± 14.0/82.0 ± 8.3 and 6.3 ± 1.7/1.5 ± 1.7). Post-operative GRF-to-tibial plateau intersection patterns were significantly ($p < 0.001$) more lateral (31.9 ± 19.8% of tibial plateau width) than the pre-operative patterns. Personalized HTO successfully and consistently lateralizes the GRF at the knee, in association with significant improvements in function and pain. The novel combination of 3D bone modelling and motion analysis also has the potential to further aid HTO surgical planning.

Keywords: high tibial osteotomy; personalized devices; medical imaging; joint modelling; gait analysis; weight-bearing CT; statistical parametric mapping

check for updates

Citation: Belvedere, C.; Gill, H.S.; Ortolani, M.; Sileoni, N.; Zaffagnini, S.; Norvillo, F.; MacLeod, A.; Dal Fabbro, G.; Grassi, A.; Leardini, A. Instrumental Gait Analysis and Tibial Plateau Modelling to Support Pre- and Post-Operative Evaluations in Personalized High Tibial Osteotomy. *Appl. Sci.* **2023**, *13*, 12425. https://doi.org/10.3390/app132212425

Academic Editor: René Schwesig

Received: 11 September 2023
Revised: 14 November 2023
Accepted: 15 November 2023
Published: 17 November 2023

Copyright: © 2023 by the authors. Licensee MDPI, Basel, Switzerland. This article is an open access article distributed under the terms and conditions of the Creative Commons Attribution (CC BY) license (https://creativecommons.org/licenses/by/4.0/).

1. Introduction

Severe varus deformity of the knee joint implies high compressive loads and cartilage wear at the medial compartment [1–4]. This condition is common in relatively young and active patients, for whom high tibial osteotomy (HTO) is indicated [5,6]. This surgical correction is intended to remove the deformity, prevent end-stage osteoarthritis [7–9] and thus delay knee replacement [10,11]. In these patients, before surgery, the mechanical axis

of the lower limb passes medially to the medial tibio-femoral condyles. During surgery, an inclined osteotomy is performed at the proximal tibia, and an open wedge is created and then stabilized with an osteosynthesis plate. After surgery, the normal alignment is usually restored, which should result in the mechanical axis passing much closer to the knee joint centre, both in standing posture and during locomotion, thus also restoring physiological joint moments and load distribution on the tibial plateau [12–14].

A limitation of the current HTO procedures is the lack of a personalized pre-operative plan for the correction. This should be based on three-dimensional (3D) bone models, because this deformity is multiplanar [15]. The clinical outcome is highly dependent upon achieving the required level of correction [16,17]. This is particularly true of current manual surgical techniques and the standard off-the-shelf plates [18], which do not match well with the surface at the tibia [19,20]. Due to these limitations, HTO is nowadays less commonly offered to varus knee patients, and complications have been reported [12,17,21,22].

With the aim of improving biomechanical and clinical results, a personalized system was developed recently [12,23–25]. An accurate 3D planning procedure based on medical imaging of the patient, including computed tomography (CT) of the knee in addition to standard weight-bearing long-leg radiographs, is performed before HTO. From the 3D planning, personalized instrumentation (the combined cutting guide and opening jig) and implant (the custom plate) are autogenerated, being designed to control, perform and then stabilize the opening-wedge osteotomy. The instrumentation and implant are then produced using additive manufacturing and delivered ready for surgery within fourteen days of the clinical confirmation of the surgical plan [12,23].

To assess the results carefully, various techniques have been exploited. Radiography provides a good measure of the correction, but it is static and limited to two dimensions [26]. Three-dimensional gait analysis is also performed [27,28], but it is based on external markers, which are largely affected by skin motion artefact. Also, the typical stick diagram connecting these markers does not show the patient-specific proximal tibial bone, which is necessary to reveal the biomechanical effects of the correction. This can be overcome by combining gait analysis with CT [25] and superimposing the ground reaction forces (GRF) onto the proximal tibial surface model from CT. In our preliminary work, a consistent post-operative shift of the GRF toward the lateral part of the tibial plateau was observed, showing that this force is generally better aligned with the mechanical axis of the lower limb after surgery.

The aim of the present study is to report an original functional analysis conducted to assess the biomechanical effects on the lower limb of a personalized procedure for HTO. This includes state-of-the-art gait analysis, medical imaging and modelling of the proximal tibia and an original procedure for matching these techniques to obtain a patient-specific knee joint model during locomotion [25]. The present study reports the complete findings for a whole cohort from the first clinical trial of this personalized HTO procedure, which was preliminary validated on a limited patient population [25]. The main hypothesis is that consistent lateralization of the GRF over the tibial plateau occurs after personalized HTO.

2. Methods

2.1. Patient Cohort

Between December 2019 and November 2022, twenty-five patients with early-stage medial knee osteoarthritis resulting from varus knee malalignment were recruited for the novel opening-wedge personalized HTO surgical procedure (Table 1). All patients received radiological and instrumental evaluations before and after surgery at a 6-month follow-up, as well as clinical scoring. All patients were assessed as suitable for HTO by a single experienced surgeon, who then performed all surgical procedures. This study received institutional review board approval (CE AVEC code: 623/2019/Disp/IOR; clinicaltrial.gov code: NCT04574570; type of study: preliminary pilot, single-centre, prospective, uncontrolled, 32-month-long study), and informed consent was obtained from all the participants.

The pre- and post-operative results reported in this study refer to all 25 patients initially recruited; there were no patient dropouts at any stage of the study.

Table 1. Demographic data.

	Mean ± SD	Min	Max
No. of patients (gender: male/female; side: left/right)	25 (19/6; 13/12)	-	-
Age (years)	54.1 ± 7.4	39	65
Weight (kg)	80.6 ± 14.8	57	113
Height (cm)	172.8 ± 8.8	156	195
Body mass index (kg/m^2)	26.9 ± 4.2	20.8	38.1
Inclusion criteria	Exclusion criteria		
Age 40–65 years	BMI ≥ 40		
BMI < 40	Patients unable to provide informed consent		
Varus deformity < 20°	Patients not compliant with post-operative rehabilitation and assessment schedules		
Diagnosis of non-inflammatory degenerative joint disease	Patients with specific diseases or disorders or with extremely poor bone quality		
Unicompartmental medial knee osteoarthritis	Other surgeries to the lower limbs		

2.2. The Customized HTO Procedure

The novel personalized system for HTO surgery used in the present work is the TOKA system (Tailored Osteotomy for Knee Alignment, Orthoscape, 3D Metal Printing LTD, Bath, UK) [23]. It was devised to provide patient-specific surgical guides and stabilization plates (Figure 1a–e), using additive manufacturing with metal powders (medical-grade titanium alloy Ti6AL4V, ASTM F136 grade 23).

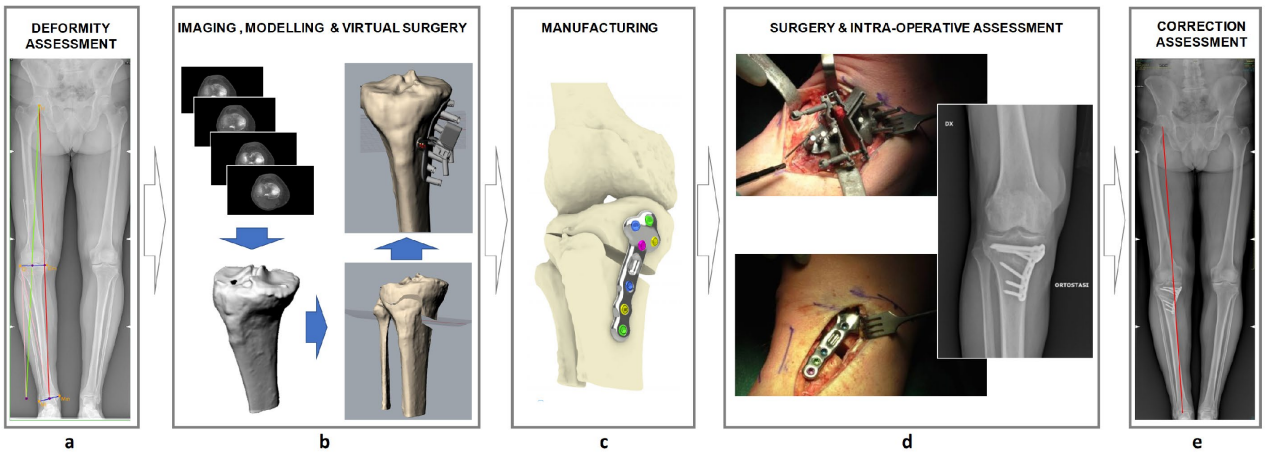

Figure 1. Workflow of the new customized HTO procedure: the original patient's deformity is assessed on a standing long-leg frontal radiograph (**a**); virtual surgery is based on a 3D anatomical model of the knee reconstructed from CT images of the patient (**b**); the HTO fixation plate is then 3D-printed in medical titanium alloy (**c**) and delivered to the hospital for sterilization and surgical implantation (**d**); the final alignment of the lower limb is assessed on another standing frontal radiograph (**e**).

In addition to the traditional weight-bearing bilateral long-leg standing radiograph, a cone beam CT scan of the knee joint was also taken in a weight-bearing position (OnSight 3D Extremity, Carestream, Rochester, NY, USA), with the patient upright in a natural single-leg standing position. From this scan, the 3D geometry of the distal femur and the proximal tibia was generated in STL format. In the same scan, knee markers for subsequent gait analysis and registration purposes [25] were also visible and reconstructed in 3D.

From the frontal plane radiograph, the desired angle of correction was calculated (where 180° was the target alignment and >180° was varus), and this was used to determine the position and opening of the osteotomy at the proximal tibia. The 3D anatomical model of the knee was used to fully plan the surgery, including the generation of the surgical guide to achieve the planned correction and the fixation plate to match the tibial bone surface after the opening-wedge procedure. The entire process and the final 3D plan were the result of a rigorous surgical planning procedure performed collaboratively by the surgeon and the implant company bioengineers. The medial–lateral intersection (hereafter referred to as ML, expressed as a percentage of the width of the tibial plateau, where ML = 0% represents the medial edge of the tibia) of the mechanical axis of the lower limb, also known as Mikulicz's line and drawn connecting the centre of the hip to the centre of the ankle [29], was calculated on the basis of the pre-operative weight-bearing long-leg radiograph.

2.3. Surgery

All surgeries were performed by a single experienced knee surgeon. Routine surgical steps for HTO were executed along with the additional steps required for the novel personalized procedure [23]. The former included supine patient positioning, tourniquet placement, k-wire insertion to mark the knee joint line, longitudinal skin incision and proper exposure of the antero-medial aspect of the proximal tibia [12]. As for the customized procedure, this involved fixation of the patient-specific surgical guide in the planned procedure, execution of the biplanar osteotomy with intraoperative radiographic control, guide removal and personalized plate fixation (Figure 1) with allograft bone used for gap filling followed by final suturing [23]. A standard rehabilitation program was then prescribed to allow a phased return to normal physical activity [30].

2.4. Clinical, Functional and Radiological Analyses

Patient-reported outcomes (PROMs) were collected pre-operatively, and at one, three, six and twelve months after surgery. These included the Knee Osteoarthritis Outcome Score (KOOS) [31], here considered as a total score averaged across all domains and as individual domains (KOOS, 0 = worst condition, 100 = best condition), and the visual analogue pain scores [32] during activity (VAS, 0 = no pain, 10 = worst pain).

Instrumented gait analysis was also performed prior to the surgery and at 6 months follow-up (Figure 2). A nine-camera motion capture system (Vicon®, Nexus motion-capture Software v.2.12.1, with B10 Bonita Optical cameras, Oxford, UK), together with two GRF-measuring platforms (KistlerTM, model 9291B, Winterthur, Switzerland) and a wireless EMG system (Zerowire, Cometa, Milan, Italy) for the myoelectric activity of the main muscles of the lower limbs were employed. An established protocol (IOR-gait) [33] with tested data reproducibility [34] and consistency [35] was used to position reflective markers on the skin in well-defined anatomical landmarks and to calculate 3D kinematics and kinetics of the hip, knee and ankle joints.

Gait analysis data were collected during five repetitions of level walking. All patients were asked to walk at their self-selected speed. The standard marker set was enriched with four additional knee-related fiduciary markers used for the subsequent medical imaging analysis, morphological reconstruction and data registration purposes (Figure 2) according to a recently reported original methodology developed by the present authors [25], where the reproducibility of the combination of stereophotogrammetric and force platform data was also assessed. Whilst the patients were still wearing these additional knee-related fiduciary markers, long-leg radiographs and cone beam CT examination were undertaken for the knee in the weight-bearing condition; this imaging was needed before surgery for the planning, as detailed above, and was repeated at 6 months follow-up. Three-dimensional bone morphological models for the tibia and the fiduciary markers were reconstructed from the CT imaging. Next, the fiduciary marker trajectories obtained from gait analysis were registered to the corresponding marker coordinates from the CT-based reconstruction, allowing superimposition of the GRF data to the reconstructed tibia morphology. A plane

matching the border of the tibial plateau was defined, and its intersections with the GRF vectors were calculated.

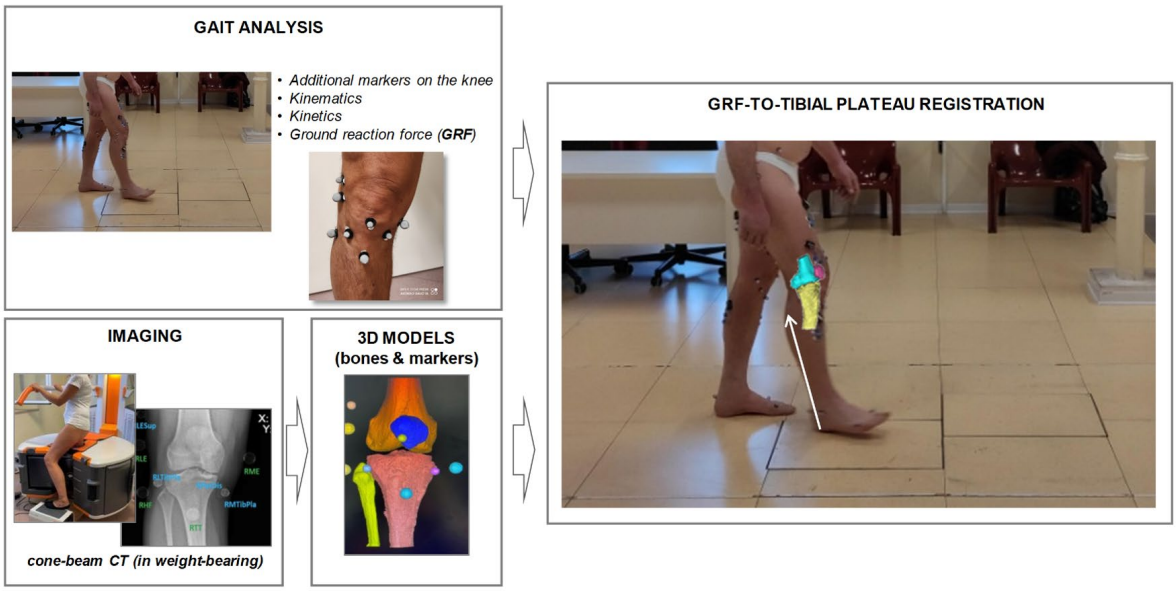

Figure 2. Workflow of the recently reported methodology for characterizing GRF data on tibial morphology [25]: functional data are collected via gait analysis during level walking, using a standard marker set protocol enriched with additional markers around the knee; medical images are acquired with CT scan, and related DICOM files are used to reconstruct 3D models for the bones and the additional markers; a single-value decomposition approach combining the reconstructed and tracked additional markers is then used to register the positions of the GRF vectors on the tibial bone model.

2.5. Data Processing and Statistical Analysis

With the proposed power of 80% and an α level of 0.05 for radiographical evaluations, a sample size of at least 25 was needed to derive significant differences between planned and post-operative alignment data, specifically the orientation of the tibial osteotomy and the mechanical axis of the lower limb. This computation assumes that the general mean difference between the two conditions was 2.0° in radiological evaluations with relevant standard deviation equal to 3.0°.

All data are presented in terms of mean ± standard deviation. In detail, pre- and post-operative 3D kinematics and kinetics of the hip, knee and ankle joints from gait analysis were calculated in degrees (°) and in % patient's body weight (BW) times height (H), and versus % of gait cycle; these were compared with reference data from the literature [33] for the level-walking task only. Pre- and post-operative ML and antero-posterior (AP) coordinates (in mm and in % of AP and ML tibial plateau dimensions) of the intersections of the GRF vectors with the tibial plateau were calculated versus % of gait cycle.

Statistical parametric mapping (SPM) [36], which has recently been applied for biomechanical analyses [37], was used for statistical comparisons between curves. The Kolmogorov–Smirnov test was applied preliminarily to check normality in data distribution; consequently, Student's *t* test or the Mann–Whitney–Wilcoxon test was utilized for data comparison between the pre- and post-operative data. Furthermore, the Pearson's product moment correlation coefficient (R) was calculated to determine the relationships between pre- and post-operative clinical and radiological scoring. In all comparisons, a *p*-value of less than 0.05 was taken to reveal statistically significant differences; otherwise, non-significance (NS) was indicated. All calculations were performed blinded to the pre/post-operative timeframe (Matlab®, R2022a The MathWorks, Inc., Natick, MA, USA).

3. Results

3.1. Overview

Pre-operative radiological evaluation in double-leg standing position and clinical scoring confirmed the diagnosis of medial knee osteoarthritis, with a mean varus deformity of 9.3 ± 3.2° on average for the 25 patients, associated with a mean total KOOS score of 56.2 ± 14.0 and a mean VAS pain on activity score of 6.3 ± 1.7. Six months after surgery, the varus deformity significantly dropped down to 2.5 ± 2.8° (R = −0.76, $p < 0.0001$), i.e., a more physiological hip–knee–ankle alignment, which was associated with an average total KOOS score of 82.0 ± 8.3 and an average VAS pain on activity score of 1.5 ± 1.7. The pre- versus post-operative changes in KOOS (R = 0.75) and VAS scores (R = −0.81) were both highly significant ($p < 0.001$). In terms of Mikulicz's line with respect to the medial ridge of the tibial plateau, the corresponding pre-operative ML distance changed significantly from a mean of 9.5 ± 13.2% pre-operatively to a mean of 39.6 ± 11.0% post-operatively (R = 0.87, $p < 0.0001$), i.e., much closer to the centre of the tibial plateau, as desired.

In gait analysis, the raw (cm/s) and normalized (% body height/s) values for the self-selected walking speed measured pre-operatively were 105.0 ± 25.4 and 61.0 ± 14.8. Post-operatively, these values became 108.7 ± 18.2 and 62.9 ± 11.2, respectively. Although not statistically significant, post-operative speed was slightly higher and more consistent among the patients.

3.2. GRF Characterization on Tibial Plateau

Using the recently reported methodology to characterize the GRF with respect to the patient-specific tibial plateau plane [25], the post-operative patterns of intersections were found to be significantly more lateral and closer to the centre of the tibial plateau than the pre-operative patterns (Figures 3 and 4), with no significant changes along the AP direction. In detail, for all analysed patients, the observed lateralization was on average 25.2 ± 16.5 mm, corresponding to a mean of 31.9 ± 19.8% in terms of the percentage of tibial plateau width. This significant change was confirmed with SPM analysis throughout the gait cycle (Figure 3), and it is consistent with the changes in Mikulicz's line position, as reported above. The total amount of lateralization for each patient was calculated as the ML difference (pre- and post-operative) of the centroid of the intersection pattern. This was found to be significantly correlated with the HTO correction angle, with lateralization expressed in both mm (R = 0.55, $p < 0.005$) and the percentage of tibial plateau width (R = 0.50, $p < 0.05$). This lateralization was also significantly correlated with the ML distance of Mikulicz's line both in mm (R = 0.55, $p < 0.05$) and percentage (R = 0.46, $p < 0.05$), respectively.

3.3. Kinematics

Comparing post-operative to pre-operative joint rotations, considerable differences were observed mostly in the frontal plane (Figure 5). In the sagittal plane, the absolute difference throughout the gait cycle was 1.7 ± 6.0° on average for the 25 patients, with no statistical significance, as revealed by SPM analysis. In the transverse plane, this value was slightly larger, 4.5 ± 7.6°, with limited significant differences in the mid/late stance for the hip and in the late stance and swing for the knee. In the frontal plane, this value was 3.8 ± 4.0°, with significant differences in the full stance for the hip and knee and throughout the whole gait cycle for the ankle. These pre- versus post-operative differences were found to be significant despite the smaller corresponding mean value in the transverse plane, which was likely because of the smaller range of rotation in the frontal plane. Overall, when compared to physiological data from the literature [33], these observed changes were always in the direction of physiological values.

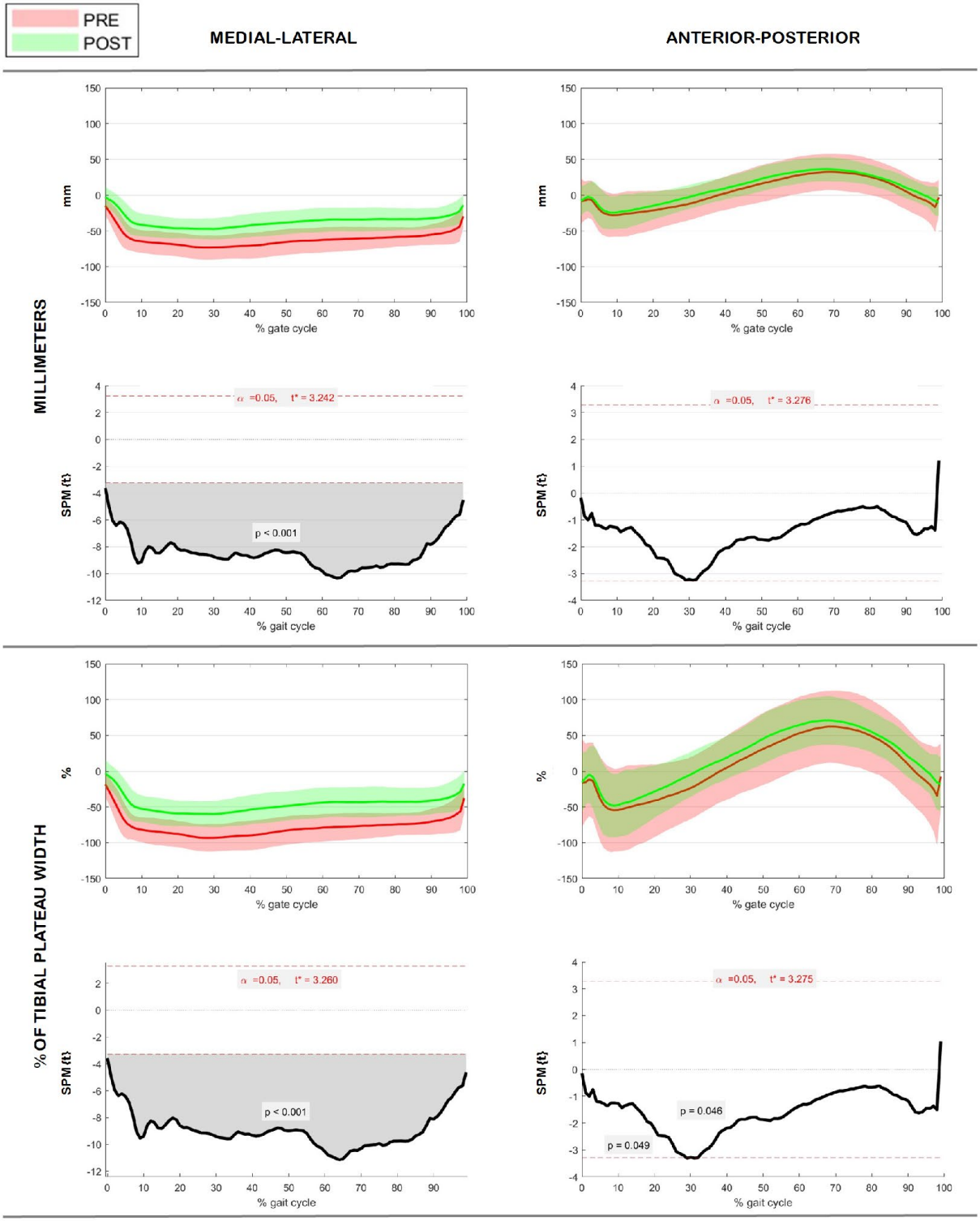

Figure 3. Medial–lateral and anterior–posterior patterns of intersections versus % of gait stance. Pre- and post-operative data are reported as mean curves ± standard deviations for all patients, both in millimetres (mm) and in % of the tibial plateau width, along with the associated comparison of pre–post data via SPM (SPM{t}), where t* indicates the critical value of t given the significance level α.

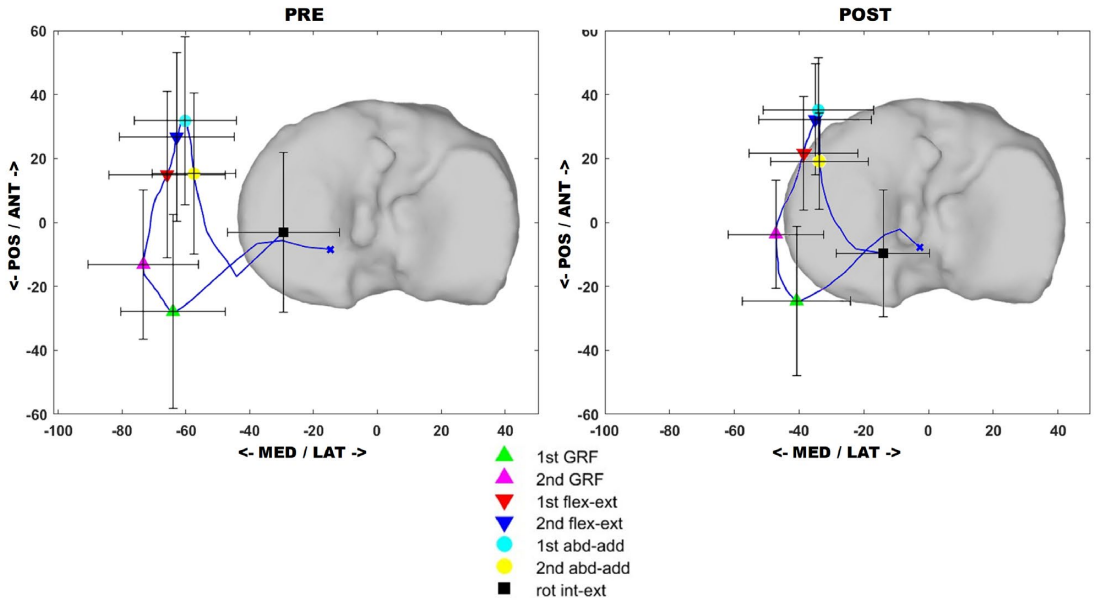

Figure 4. Mean pre- and post-operative pattern of intersections (in mm) superimposed on the 3D tibial plateau model from a representative patient (transverse view in the tibial anatomical reference frame) compared with all patients. The standard deviations in the AP and ML direction associated with the first and the second GRF peak in the stance phase (1st and 2nd GRF) to the first and the second sagittal (1st and 2nd flex-ext) and frontal (1st and 2nd abd-add) knee moment peaks and to the transverse knee moment peak (int-ext) are also shown.

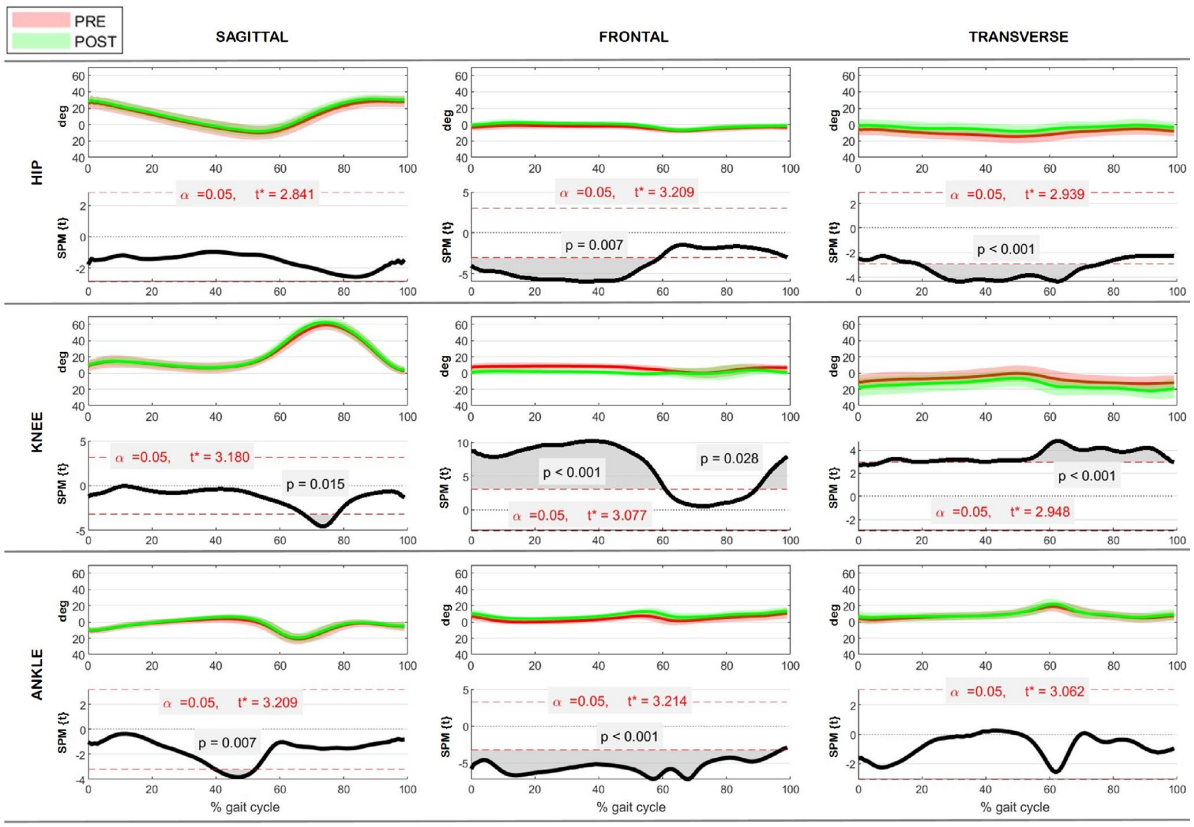

Figure 5. Hip, knee and ankle joint kinematics on the sagittal, frontal and transverse plane versus % of gait cycle. Pre- and post-operative rotations (in degrees) are reported as mean curves ± standard deviations for all patients, along with the associated comparison of pre–post data via SPM (SPM{t}), where t* indicates the critical value of t given the significance level α.

3.4. Kinetics

Comparing post-operative to pre-operative joint moments, again, considerable differences were observed mostly in the frontal plane for the knee (Figure 6). In the sagittal plane, the absolute difference throughout the gait cycle was 0.2 ± 1.0%BW × H on average for the 25 patients, with no statistical differences, apart from in the late stance for the ankle, as revealed by SPM. In the transverse plane, this value was 0.1 ± 0.2%BW × H, with significant differences in mid-stance for the hip and knee. In the frontal plane, a difference of 1.0 ± 0.8%BW × H was observed only for the knee, with statistical significance in the full stance. Overall, for kinetic data, when compared to physiological data from the literature [33], these observed changes were also always in the direction of physiological values.

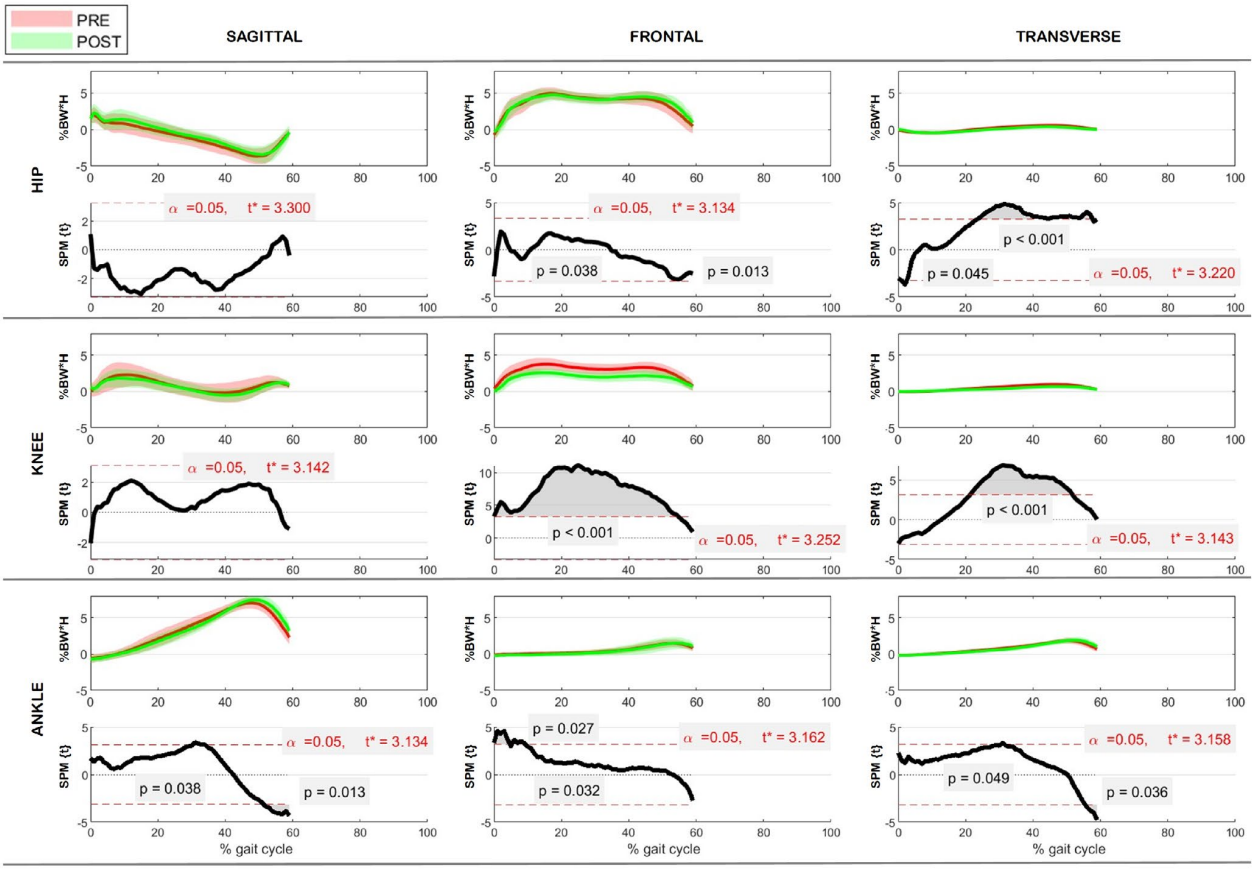

Figure 6. Hip, knee and ankle joint kinetics on the sagittal, frontal and transverse plane versus % of the full gait cycle (stance phase, i.e., with the foot on the forceplate, finishing at about 60% of the cycle). Pre- and post-operative data (in %BWxH) are reported as mean curves ± standard deviations for all patients, along with the associated comparison of pre–post data via SPM (SPM{t}), where t* indicates the critical value of t given the significance level α.

4. Discussion

The present work reports the results of a complete clinical trial using an original multi-instrument procedure to assess the biomechanical effects on the operated lower limb for a novel custom-made HTO system for the personalized surgical correction of large knee varus deformities.

Outcomes according to medical imaging and clinical scores before and after HTO are reported, but mainly a thorough functional assessment was performed and discussed. This involved merging state-of-the-art gait analysis with individual knee bone models from CT scans taken in a weight-bearing position. The fully personalized surgical procedure should have guaranteed relevant biomechanical correction at the knee as well as at the hip and ankle joints. A considerable consistent improvement at these joints in all three

anatomical planes was observed, supported also by a thorough statistical analysis of the whole gait cycle in level walking. From the original procedure, patient-specific patterns of GRF location on the tibial plateau were obtained from the foot strike to toe off.

A number of previous papers have used standard gait analysis to assess kinematics and kinetics at the major joints of the lower limbs for HTO patients [27,38–40]. The present procedure also originally included state-of-the-art technology to enhance skeletal modelling of the knee bones by using a modern cone beam CT scanner. This enables 3D reconstruction of bone segments in a weight-bearing position for a realistic full representation of the knee morphology and alignment [41,42]. Though the correction angle for the present surgical intervention was determined only from the long-leg frontal radiograph, the 3D model of the distal femur, of the patella and of the proximal tibia supported the best possible location and orientation of the osteotomy, also including possible necessary realignments out of the frontal plane [23]. An overall high-accuracy realignment is expected to be enabled by the cutting jig and the plate, which were both designed to match the tibial bones and to accurately achieve the desired correction. A robust stabilization of the open wedge was also expected. Thus, the present thorough functional analysis was performed on patients who underwent a highly optimized HTO intervention. The present results show a good restoration after surgery not only of traditional radiographical alignment but also of the physiological kinematics and kinetics of the knee and the other joints of the operated lower limb. These findings concur with those reported in the literature regarding the positive effects of using customized approaches in HTO, such as subject-specific cutting jigs [43,44], both in terms of knee joint line realignment and clinical outcomes. In addition, though the actual association between post-operative joint line correction and the clinical consequences after HTO for medial knee osteoarthritis apparently cannot yet be ascertained from the recent literature [45–47], the present post-operative clinical scores demonstrate overall significant improvements for the treated patients in terms of pain relief and normal gait restoration after surgery.

One of the major claims of opening-wedge HTO is a lateral transfer of loads for a relevant decompression of the medial compartment of the varus knee, which allows for improved mediolateral weight distribution at the tibial plateau and a more steady and symmetrical overall posture [12–14]. This is usually shown by reporting the time–history of the ab/adduction moment of the knee from traditional gait analysis [1,28,33]. This reveals the distance of the GRF vector from the knee joint centre in the mediolateral direction. The present technique can reveal the exact location of the GRF vectors in the plane of the tibial plateau of the subject throughout the stance phase of walking. Though the relevant patterns were found to be patient-specific, these can reveal better overall compensatory mechanisms of knee joint off-loading with an effective graphical representation. The only previous similar work [28] was limited to only two moments in time, i.e., the first and second peak of the knee ab/adduction moment, and to a generic non-subject-specific definition of the virtual tibial plateau.

The novel combination of 3D joint surface modelling and motion analysis data allows a direct visualization of the direct biomechanical consequences of the surgical procedure. Performing this type of assessment in a larger cohort will provide an opportunity to explore the relationship between degree of correction and the amount of GRF lateralization achieved. Surgeons are concerned about changing the posterior slope of the tibial surface and have proposed the biomechanical consequences of doing so. The assessment technique described is able to determine the effects of tibial surface slope change on the GRF intersection.

This study is not free from limitations. The clinical trial population size was not very large, but the technique implies an invasive CT scan, not a standard pre- or post-operative assessment in HTO; however, the present statistical analysis has the necessary power, and cone beam CT is less invasive than standard CT [41]. The degree of deformity and correction varied considerably for the analysed patients; this may be considered a weakness of the study, but also a strength after the final observation of consistent amelioration of the joint biomechanics in all cases, i.e., independently of the condition pre-op. The best-

matching plane to virtually represent the tibial plateau can be defined in many different ways; however, a preliminary sensitivity analysis revealed that the relevant effect on the pre- vs. post-op differences for the intersections patterns was very small [25]. The present dataset from the overall technique, which merges gait analysis and 3D modelling, does not have a corresponding control from normal subjects, because of the invasive CT scans. To address this, a specialized marker set can be devised in the future to define a virtual transverse plane rigid with the tibial plateaus. Level walking was the only motor task analysed here, although preliminary observations in a limited number of patients showed similar trends in other tasks of daily living [25]. Furthermore, in the current study, the HTO planning was performed based on long-leg radiographs and CT scans, i.e., pre-operative motion analysis and GRF visualization were not used in the planning process. In the literature, as far as we could determine, there is not a single study using gait analysis to support HTO planning. A future direction for this surgery would be to exploit the presented combined modelling/motion analysis technique to improve the planning procedure utilizing patient-specific biomechanical observations and measurements.

5. Conclusions

In this work, an original multi-instrument procedure was used to show that the biomechanical effects of a carefully performed surgical realignment of knee varus deformity, i.e., open-wedge HTO, are satisfactory, and thus a transfer of loads from the medial compartment was achieved at this joint. With this medial compartment decompression and a physiological load distribution over the tibial plateau, a slowdown of the progression of osteoarthritis should also have been accomplished.

Author Contributions: C.B.: Conceptualization, Formal Analysis, Investigation, Methodology, Project Administration, Supervision, Validation, Writing—Original Draft, Writing—Review and Editing. H.S.G.: Conceptualization, Formal Analysis, Investigation, Methodology, Validation, Writing—Review and Editing. M.O.: Data Curation, Formal Analysis, Investigation, Writing—Review and Editing. N.S.: Data Curation, Formal Analysis, Investigation, Writing—Review and Editing. S.Z.: Funding Acquisition, Resources, Writing—Review and Editing. F.N.: Data Curation, Investigation, Writing—Review and Editing. A.M.: Software, Visualization, Validation, Writing—Review and Editing. G.D.F.: Data Curation, Investigation, Writing—Review and Editing. A.G.: Investigation, Writing—Review and Editing. A.L.: Conceptualization, Formal Analysis, Funding Acquisition, Project Administration, Resources, Supervision, Validation, Writing—Original Draft, Writing—Review and Editing. All authors have read and agreed to the published version of the manuscript.

Funding: This study was partially funded by the Italian Ministry of Health under the "5 per mille" program.

Institutional Review Board Statement: This study was approved by the Ethics Committee (Prot. Gen. 0013355 on 30 October 2019) of the IRCCS Istituto Ortopedico, BolognaItaly (Cod. CE AVEC: 623/2019/Disp/IOR) and the clinical trial was registered at *ClinicalTrials.gov* (Cod.: NCT04574570). The authors certify that the institution approved the investigation protocol, that all investigations were conducted in conformity with ethical standard of research and in accordance with the relevant guidelines and regulations.

Informed Consent Statement: Informed consent was obtained from all subjects involved in the study.

Data Availability Statement: Data presented in this study are available upon reasonable request to the corresponding author. The data are not publicly available for privacy reasons.

Conflicts of Interest: Gill and MacLeod are the named inventors on the personalized device patent. All other authors declare that there they have no personal or commercial relationships that would lead to a conflict of interest.

References

1. Baliunas, A.J.; Hurwitz, D.E.; Ryals, A.B.; Karrar, A.; Case, J.P.; Block, J.A.; Andriacchi, T.P. Increased knee joint loads during walking are present in subjects with knee osteoarthritis. *Osteoarthr. Cartil.* **2002**, *10*, 573–579. [CrossRef] [PubMed]
2. Rajgopal, A.; Noble, P.C.; Vasdev, A.; Ismaily, S.K.; Sawant, A.; Dahiya, V. Wear Patterns in Knee Articular Surfaces in Varus Deformity. *J. Arthroplast.* **2015**, *30*, 2012–2016. [CrossRef]
3. Sharma, L. The role of varus and valgus alignment in knee osteoarthritis. *Arthritis Rheumatol.* **2007**, *56*, 1044–1047. [CrossRef] [PubMed]
4. Sharma, L.; Song, J.; Dunlop, D.; Felson, D.; Lewis, C.E.; Segal, N.; Torner, J.; Cooke, T.D.; Hietpas, J.; Lynch, J.; et al. Varus and valgus alignment and incident and progressive knee osteoarthritis. *Ann. Rheum. Dis.* **2010**, *69*, 1940–1945. [CrossRef]
5. Khakha, R.S.; Bin Abd Razak, H.R.; Kley, K.; van Heerwaarden, R.; Wilson, A.J. Role of high tibial osteotomy in medial compartment osteoarthritis of the knee: Indications, surgical technique and outcomes. *J. Clin. Orthop. Trauma* **2021**, *23*, 101618. [CrossRef] [PubMed]
6. Wolcott, M.; Traub, S.; Efird, C. High tibial osteotomies in the young active patient. *Int. Orthop.* **2010**, *34*, 161–166. [CrossRef]
7. Jackson, J.P.; Waugh, W. Tibial osteotomy for osteoarthritis of the knee. *J. Bone Jt. Surg. Br.* **1961**, *43-B*, 746–751. [CrossRef]
8. Lee, D.C.; Byun, S.J. High tibial osteotomy. *Knee Surg. Relat. Res.* **2012**, *24*, 61–69. [CrossRef]
9. Rossi, R.; Bonasia, D.E.; Amendola, A. The Role of High Tibial Osteotomy in the Varus Knee. *JAAOS J. Am. Acad. Orthop. Surg.* **2011**, *19*, 590–599. [CrossRef]
10. Fujisawa, Y.; Masuhara, K.; Shiomi, S. The effect of high tibial osteotomy on osteoarthritis of the knee. An arthroscopic study of 54 knee joints. *Orthop. Clin. N. Am.* **1979**, *10*, 585–608. [CrossRef]
11. Primeau, C.A.; Birmingham, T.B.; Leitch, K.M.; Willits, K.R.; Litchfield, R.B.; Fowler, P.J.; Marsh, J.D.; Chesworth, B.M.; Dixon, S.N.; Bryant, D.M.; et al. Total knee replacement after high tibial osteotomy: Time-to-event analysis and predictors. *CMAJ* **2021**, *193*, E158–E166. [CrossRef] [PubMed]
12. Zaffagnini, S.; Dal Fabbro, G.; Belvedere, C.; Leardini, A.; Caravelli, S.; Lucidi, G.A.; Agostinone, P.; Mosca, M.; Neri, M.P.; Grassi, A. Custom-Made Devices Represent a Promising Tool to Increase Correction Accuracy of High Tibial Osteotomy: A Systematic Review of the Literature and Presentation of Pilot Cases with a New 3D-Printed System. *J. Clin. Med.* **2022**, *11*, 5717. [CrossRef] [PubMed]
13. Brehme, K.; Bartels, T.; Pyschik, M.; Jenz, M.; Delank, K.S.; Laudner, K.G.; Schwesig, R. Postural stability and regulation before and after high tibial osteotomy and rehabilitation. *Appl. Sci.* **2020**, *10*, 6517. [CrossRef]
14. Kurz, E.; Brehme, K.; Bartels, T.; Pyschik, M.; Jenz, M.; Kadler, W.; Delank, K.S.; Schwesig, R. Standing Steadiness and Asymmetry after High Tibial Osteotomy Surgery: A 2 Year Follow-Up Study. *J. Pers. Med.* **2022**, *12*, 1594. [CrossRef] [PubMed]
15. Laven, I.; Schroder, F.F.; de Graaff, F.; Rompen, J.C.; Hoogeslag, R.A.G.; van Houten, A.H. Accuracy, inter- and intrarater reliability, and user-experience of high tibial osteotomy angle measurements for preoperative planning: Manual planning PACS versus semi-automatic software programs. *J. Exp. Orthop.* **2022**, *9*, 44. [CrossRef]
16. Hsu, R.W.; Himeno, S.; Coventry, M.B.; Chao, E.Y. Normal axial alignment of the lower extremity and load-bearing distribution at the knee. *Clin. Orthop. Relat. Res.* **1990**, *255*, 215–227. [CrossRef]
17. Spahn, G. Complications in high tibial (medial opening wedge) osteotomy. *Arch. Orthop. Trauma Surg.* **2004**, *124*, 649–653. [CrossRef]
18. Diffo Kaze, A.; Maas, S.; Waldmann, D.; Zilian, A.; Dueck, K.; Pape, D. Biomechanical properties of five different currently used implants for open-wedge high tibial osteotomy. *J. Exp. Orthop.* **2015**, *2*, 14. [CrossRef]
19. Brouwer, R.W.; Bierma-Zeinstra, S.M.; van Raaij, T.M.; Verhaar, J.A. Osteotomy for medial compartment arthritis of the knee using a closing wedge or an opening wedge controlled by a Puddu plate. A one-year randomised, controlled study. *J. Bone Jt. Surg. Br.* **2006**, *88*, 1454–1459. [CrossRef]
20. Woodacre, T.; Ricketts, M.; Evans, J.T.; Pavlou, G.; Schranz, P.; Hockings, M.; Toms, A. Complications associated with opening wedge high tibial osteotomy—A review of the literature and of 15 years of experience. *Knee* **2016**, *23*, 276–282. [CrossRef]
21. Han, S.B.; In, Y.; Oh, K.J.; Song, K.Y.; Yun, S.T.; Jang, K.M. Complications Associated with Medial Opening-Wedge High Tibial Osteotomy Using a Locking Plate: A Multicenter Study. *J. Arthroplast.* **2019**, *34*, 439–445. [CrossRef] [PubMed]
22. Murray, R.; Winkler, P.W.; Shaikh, H.S.; Musahl, V. High Tibial Osteotomy for Varus Deformity of the Knee. *J. Am. Acad. Orthop. Surg. Glob. Res. Rev.* **2021**, *5*, e21.00141. [CrossRef]
23. Belvedere, C.; MacLeod, A.; Leardini, A.; Grassi, A.; Dal Fabbro, G.; Zaffagnini, S.; Gill, H.S. 3D medical imaging analysis, patient-specific instrumentation and individualized implant design, with additive manufacturing creates a new personalized high tibial osteotomy treatment option. *J. Mech. Med. Biol.* **2023**, *23*, 2340041. [CrossRef]
24. MacLeod, A.; Belvedere, C.; Dal Fabbro, G.; Grassi, A.; Nervuti, G.; Leardini, A.; Casonato, A.; Zaffagnini, S.; Gill, H.S. First Clinical Experience of a Personalised 3D-Printed Osteotomy System for Knee Arthritis Treatment. In Proceedings of the British Orthopaedic Research Society Annual Meeting, Online, 13–14 September 2021.
25. Ruggeri, M.; Gill, H.S.; Leardini, A.; Zaffagnini, S.; MacLeod, A.; Ortolani, M.; Faccia, F.; Grassi, A.; Fabbro, G.D.; Durante, S.; et al. Superimposition of ground reaction force on tibial-plateau supporting diagnostics and post-operative evaluations in high-tibial osteotomy. A novel methodology. *Gait Posture* **2022**, *94*, 144–152. [CrossRef] [PubMed]
26. Li, O.L.; Pritchett, S.; Giffin, J.R.; Spouge, A.R.I. High Tibial Osteotomy: An Update for Radiologists. *AJR Am. J. Roentgenol.* **2022**, *218*, 701–712. [CrossRef]

27. Lee, S.H.; Lee, O.S.; Teo, S.H.; Lee, Y.S. Change in gait after high tibial osteotomy: A systematic review and meta-analysis. *Gait Posture* **2017**, *57*, 57–68. [CrossRef]
28. Whatling, G.M.; Biggs, P.R.; Elson, D.W.; Metcalfe, A.; Wilson, C.; Holt, C. High tibial osteotomy results in improved frontal plane knee moments, gait patterns and patient-reported outcomes. *Knee Surg. Sports Traumatol. Arthrosc.* **2020**, *28*, 2872–2882. [CrossRef]
29. Marques Luis, N.; Varatojo, R. Radiological assessment of lower limb alignment. *EFORT Open Rev.* **2021**, *6*, 487–494. [CrossRef]
30. Aalderink, K.J.; Shaffer, M.; Amendola, A. Rehabilitation following high tibial osteotomy. *Clin. Sports Med.* **2010**, *29*, 291–301. [CrossRef]
31. Roos, E.M.; Lohmander, L.S. The Knee injury and Osteoarthritis Outcome Score (KOOS): From joint injury to osteoarthritis. *Health Qual. Life Outcomes* **2003**, *1*, 64. [CrossRef]
32. Delgado, D.A.; Lambert, B.S.; Boutris, N.; McCulloch, P.C.; Robbins, A.B.; Moreno, M.R.; Harris, J.D. Validation of Digital Visual Analog Scale Pain Scoring with a Traditional Paper-based Visual Analog Scale in Adults. *J. Am. Acad. Orthop. Surg. Glob. Res. Rev.* **2018**, *2*, e088. [CrossRef]
33. Leardini, A.; Sawacha, Z.; Paolini, G.; Ingrosso, S.; Nativo, R.; Benedetti, M.G. A new anatomically based protocol for gait analysis in children. *Gait Posture* **2007**, *26*, 560–571. [CrossRef]
34. Manca, M.; Leardini, A.; Cavazza, S.; Ferraresi, G.; Marchi, P.; Zanaga, E.; Benedetti, M.G. Repeatability of a new protocol for gait analysis in adult subjects. *Gait Posture* **2010**, *32*, 282–284. [CrossRef] [PubMed]
35. Benedetti, M.G.; Merlo, A.; Leardini, A. Inter-laboratory consistency of gait analysis measurements. *Gait Posture* **2013**, *38*, 934–939. [CrossRef] [PubMed]
36. Friston, K.J.; Ashburner, J.T.; Kiebel, S.J.; Nichols, T.E.; Penny, W.D. *Statistical Parametric Mapping: The Analysis of Functional Brain Images*; Elsevier/Academic Press: Amsterdam, The Netherlands, 2007.
37. Pataky, T.C. Generalized n-dimensional biomechanical field analysis using statistical parametric mapping. *J. Biomech.* **2010**, *43*, 1976–1982. [CrossRef]
38. Lind, M.; McClelland, J.; Wittwer, J.E.; Whitehead, T.S.; Feller, J.A.; Webster, K.E. Gait analysis of walking before and after medial opening wedge high tibial osteotomy. *Knee Surg. Sports Traumatol. Arthrosc.* **2013**, *21*, 74–81. [CrossRef]
39. Liu, X.; Chen, Z.; Gao, Y.; Zhang, J.; Jin, Z. High Tibial Osteotomy: Review of Techniques and Biomechanics. *J. Healthc. Eng.* **2019**, *2019*, 8363128. [CrossRef]
40. Morin, V.; Pailhe, R.; Duval, B.R.; Mader, R.; Cognault, J.; Rouchy, R.C.; Saragaglia, D. Gait analysis following medial opening-wedge high tibial osteotomy. *Knee Surg. Sports Traumatol. Arthrosc.* **2018**, *26*, 1838–1844. [CrossRef]
41. Leardini, A.; Durante, S.; Belvedere, C.; Caravaggi, P.; Carrara, C.; Berti, L.; Lullini, G.; Giacomozzi, C.; Durastanti, G.; Ortolani, M.; et al. Weight-bearing CT Technology in Musculoskeletal Pathologies of the Lower Limbs: Techniques, Initial Applications, and Preliminary Combinations with Gait-Analysis Measurements at the Istituto Ortopedico Rizzoli. *Semin. Musculoskelet. Radiol.* **2019**, *23*, 643–656. [CrossRef]
42. Turmezei, T.D.; Low, S.B.; Rupret, S.; Treece, G.M.; Gee, A.H.; MacKay, J.W.; Lynch, J.A.; Poole, K.E.; Segal, N.A. Multiparametric 3-D analysis of bone and joint space width at the knee from weight bearing computed tomography. *Osteoarthr. Imaging* **2022**, *2*, 100069. [CrossRef]
43. Dasari, S.P.; Hevesi, M.; Mameri, E.; Ferrer-Rivero, R.; Fortier, L.M.; Jackson, G.R.; Warrier, A.A.; Maheshwer, B.; Jawanda, H.; Khan, Z.A.; et al. Patient-specific instrumentation for medial opening wedge high tibial osteotomies in the management of medial compartment osteoarthritis yields high accuracy and low complication rates: A systematic review. *J. ISAKOS* **2023**, *8*, 163–176. [CrossRef] [PubMed]
44. Pang, R.; Jiang, Z.; Xu, C.; Shi, W.; Zhang, X.; Wan, X.; Bahat, D.; Li, H.; Senatov, F.; Bulygina, I.; et al. Is Patient-Specific Instrumentation Accurate and Necessary for Open-Wedge High Tibial Osteotomy? A Meta-Analysis. *Orthop. Surg.* **2023**, *15*, 413–422. [CrossRef] [PubMed]
45. Akamatsu, Y.; Kumagai, K.; Kobayashi, H.; Tsuji, M.; Saito, T. Effect of Increased Coronal Inclination of the Tibial Plateau After Opening-Wedge High Tibial Osteotomy. *Arthroscopy* **2018**, *34*, 2158–2169.e2. [CrossRef]
46. Kim, C.W.; Seo, S.S.; Lee, C.R.; Gwak, H.C.; Kim, J.H.; Jung, S.G. Factors affecting articular cartilage repair after open-wedge high tibial osteotomy. *Knee* **2017**, *24*, 1099–1107. [CrossRef] [PubMed]
47. Xie, T.; Brouwer, R.W.; van den Akker-Scheek, I.; van der Veen, H.C. Clinical relevance of joint line obliquity after high tibial osteotomy for medial knee osteoarthritis remains controversial: A systematic review. *Knee Surg. Sports Traumatol. Arthrosc.* **2023**, *31*, 4355–4367. [CrossRef] [PubMed]

Disclaimer/Publisher's Note: The statements, opinions and data contained in all publications are solely those of the individual author(s) and contributor(s) and not of MDPI and/or the editor(s). MDPI and/or the editor(s) disclaim responsibility for any injury to people or property resulting from any ideas, methods, instructions or products referred to in the content.